Temperature and sample dependence of the binding free energies of complexes in crystals: The case of acceptor-oxygen complexes in Si

M. Sanati and S. K. Estreicher*
Physics Department, Texas Tech University, Lubbock, Texas 79409-1051, USA
(Received 21 June 2005; revised manuscript received 24 August 2005; published 28 October 2005)

The binding free energy E_b of a complex $\{A,B\}$ in a crystal varies not only with temperature but also the concentrations of the constituent species A and B in the sample. Except at very low temperatures, $E_b(T)$ is a linear function of T with a slope determined by the configurational entropy and free energy terms. This is quantitatively illustrated for acceptor-oxygen complexes in Si. First principles calculations establish their structures, vibrational spectra, binding energies at $T=0$ K, and electrical activities. The temperature-dependence is obtained from (Helmholtz) vibrational free energies and configurational entropies. E_b varies much more with temperature for complexes involving species that are present in low concentrations than in high concentrations. The implications of these predictions are discussed.

DOI: 10.1103/PhysRevB.72.165206 PACS number(s): 61.72.−y, 65.40.Gr, 71.55.Cn

I. INTRODUCTION

Defects (impurities, native defects, and combinations of them) affect the mechanical, electrical, optical, and/or magnetic properties of materials, especially semiconductors.[1–3] Defects that are isolated at low temperatures often diffuse and form pairs, larger complexes, or extended precipitates upon annealing, electron irradiation, and other external factors. It is not unusual for the properties of a sample to depend on its history.

Czochralski-grown (CZ) Si contains about 10^{18} cm^{-3} interstitial oxygen (O_i). Its activation energy for diffusion is 2.5 eV.[4] Upon annealing around 450 °C, $\{O_i\}_2$ dimers form and migrate with an activation energy of 1.3 eV in the 0 charge state.[5,6] In p type material, the dimers are predicted[7] to have the charge +2 and diffuse with 0.86 eV activation energy. In the presence of minority carriers, the migration barrier drops to 0.3 eV (Ref. 7) as $\{O_i\}_2$ undergoes Bourgoin-Corbett[8] minority carrier enhanced diffusion. In various temperature ranges, these dimers play a critical role in the precipitation of oxygen (thermal donors and other aggregates) and/or interact with other defects, leading for example to the formation of boron-oxygen complexes.

A key parameter in the association and dissociation of defect pairs or larger complexes is the binding energy. At $T=0$ K, it can be calculated accurately from first principles in periodic supercells using density functional theory.[3] Such calculations give the potential energy difference ΔU between supercells containing the complex $\{A,B\}$ and the dissociated products A and B, all in the appropriate equilibrium configurations and charge states. The difference of total zero-point energy is often ignored. A and B can be isolated impurities or defects, or combinations of them. A qualitative potential energy profile is shown in Fig. 1. Of course, neither the association nor the dissociation reactions occur at $T=0$ K, the temperature at which typical calculations are performed.

The theory of reactions[9,10] and the phenomenological modeling of interconversion rates for complexes in semiconductors[11] have been discussed a long time ago and are not the focus of the present work. Instead, we calculate free energies from first principles and use a specific example (acceptor-oxygen complexes in Si) to provide numbers for the vibrational free energies as well as the configuration entropies in situations where vastly different concentrations of defects are involved.

A typical procedure to investigate dissociation reactions involves annealing experiments. A sample containing the $\{A,B\}$ complex is characterized at low temperatures using for example a deep level transient spectroscopy (DLTS) or infrared absorption (IR) signal with measurable intensity $I(0)$. The sample is then annealed for various lengths of time t at a fixed temperature T_0. The measured drop in the intensity of the signal $I(t)/I(0)$ provides the dissociation rate at the temperature T_0. The results obtained at various temperatures are fitted to $R\exp -E_d/k_BT$. An Arrhenius plot (logarithm of this function vs inverse temperature) gives a straight line, the slope of which is $-E_d/k_B$ and the intercept of which (for $T\rightarrow\infty$) is the logarithm of the dissociation rate. Such experi-

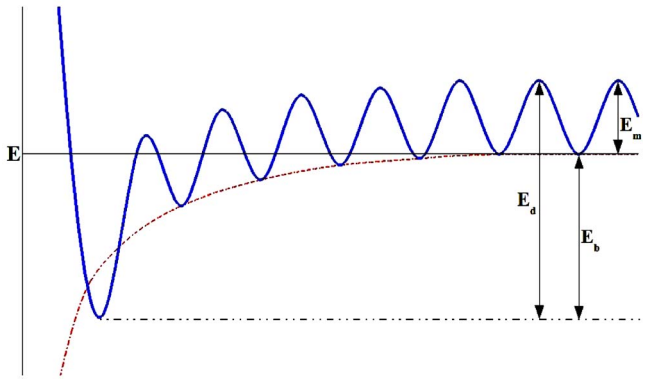

FIG. 1. (Color online) A schematic potential energy profile associated with the association or dissociation of a complex $\{A,B\}$. The long-range attractive potential (dashed curve, red) may be caused by a Coulomb or dipole interaction, or simply a strain field. The diffusing species A hops from one site to the next as it approaches B until the complex forms at the lowest-energy point. The dissociation (E_d), binding (E_b), and migration (E_m) energies are shown.

 ©2005 The American Physical Society

ments can only be performed in a narrow range of temperatures. Indeed, if the annealing temperature is too low, the complex does not dissociate in reasonable anneal times. If the temperature is too high, $\{A,B\}$ dissociates so fast that impossibly short anneal (then cool) times are required for quantitative monitoring. A recent example of this procedure is the substitutional-interstitial copper pair in Si, measured[12] in the range 333–417 K. Note that the simple process outlined above ignores the temperature range where the dissociation and association reactions compete and only a fraction of the $\{A,B\}$ complexes are bound. Although the results discussed in this paper could be extended to this general situation, the basic arguments remain the same and we will only consider the "low-T" limit where all the possible $\{A,B\}$ complexes form and the "high-T" limit where all of them are dissociated.

The binding free energy of an $\{A,B\}$ complex in a crystal is $E_b=\Delta U+\Delta F-T\Delta S_{config}$, where F is the total free energy and S_{config} the configurational entropy. E_b is not constant but varies with the temperature and the concentration of isolated A and B species in the sample. The total free energy can include a number of contributions. In special cases such as interstitial H_2 molecular impurities, the rotational term must be included.[13] When the $\{A,B\}$ and A far from B configurations lead to different free carrier concentrations, the associated change in free energy should be considered as well. However, the former is not present for the complexes considered here and the latter has recently been shown[13] to give very small contributions under all but the most extreme situations. In this paper, we consider only the vibrational free energy F_{vib} which is always present since A, B, and $\{A,B\}$ have different vibrational properties. The vibrational free energy difference between the complex and the dissociated species is temperature-dependent. Further, A, B, as well as $\{A,B\}$ are stable at specific sites in the crystal. The configurational entropies depend not just on the spin-orientational degeneracies but, more importantly, on the number of sites available and the number of A and B species present. This contribution to E_b depends on the concentrations of A and B in the sample and dominates the interactions at higher temperatures.

In Sec. II, we summarize the key features of acceptor-oxygen interactions and the theoretical results published to date. Section III deals with the methodology used in the calculations. In Sec. IV, we first compare our $T=0$ K results to those obtained by other authors, then discuss the energetics at finite temperatures. The key results are summarized and discussed in Sec. V.

II. ACCEPTOR-OXYGEN COMPLEXES IN SI: BACKGROUND

Substitutional boron (B_s) is the most common p type dopant in Si while O_i is the dominant impurity in CZ-Si, with $[O_i]>10^{18}$ cm^{-3}. Although neither B_s not O_i diffuse up to rather high temperatures, at least two types of B-O complexes have been observed to form in the 300–400 K range following irradiation or exposure to light. These defects reduce the free carrier concentration and are blamed for a $\sim$10% (relative) efficiency reduction in both space-based and terrestrial-based solar cells.[14]

In irradiated samples (typically, 1 MeV electrons), the generated self-interstitials[15] interact with B_s and create the fast-diffusing interstitial B_i.[16] The latter is characterized by an acceptor level[17] at $E_c-0.43$ eV which anneals out at 240 K at the rate $10^7\exp\{-0.6\text{ eV}/k_BT\}\text{s}^{-1}$. This suggests B_i migration with $E_m=0.6$ eV. The loss of the B_i line at $E_c-0.43$ eV correlates[18] with the growth of a defect near $E_c-0.23$ eV, the $\{B_i,O_i\}$ complex. Its gap level has also been reported at $E_c-0.27$ eV by DLTS,[16,19,20] $E_c-0.30$ eV by Hall effect[21] and in the range $E_c-0.26$ eV to $E_c-0.30$ eV by photoluminescence (PL), via the temperature dependence of the bandwidth.[22,23] The PL line at 0.87 eV has been associated with the $\{B_i,O_i\}$ pair. The thermal stability of $\{B_i,O_i\}$ is around 200 °C.[19,23] It anneals at the rate[19] $1.5\times10^{11}\exp\{-1.2\text{ eV}/k_BT\}\text{s}^{-1}$ suggesting that the complex dissociates with $E_d=1.2$ eV. This acceptor-oxygen pair is not seen in Al-doped or Ga-doped material. It is also not observed in nonirradiated samples, in which light-induced degradation is observed.[23]

The properties of $\{B_i,O_i\}$ have been calculated from first principles by Adey *et al.*[24,25] We find their structure to be metastable, albeit very close in energy to ours (see below). Their binding energy, 0.6 eV, added to the measured activation energy for diffusion of B_i, also 0.6 eV, leads to a dissociation energy of 1.2 eV, exactly the one obtained from isothermal anneals, 1.2 ± 0.1 eV.[19] Their calculated donor level is at $E_c-0.22$ eV, close to the range of the electrically active level reported by various groups, $E_c-0.23$ eV to -0.30 eV.

In samples exposed to band gap light, different reactions occurs. Few B_i's are available and almost all of the oxygen in the sample consists of isolated O_i, which has a high migration energy, 2.5 eV.[4] However, the samples also contain a small fraction of oxygen in the form of $\{O_i\}_2$ dimers. It has been shown by minority carrier lifetime spectroscopy that the concentration of the light-induced defect is proportional to the concentration of B_s (Refs. 26–28) and the square of the concentration of O_i,[27,29] suggesting a $B_s+\{O_i\}_2$ interaction. The formation of the defect involves an activation energy of 0.37 eV, and the gap level of the defect has recently been determined by advanced lifetime spectroscopy[30] to be at $E_c-0.41$ eV. The complex anneals out at 200 °C with an activation energy of 1.3 eV.[27,31] The degradation also occurs in the dark when a forward bias is applied,[32] but is not observed in Ga-doped material.[33]

A quantitative model for the formation of the light-induced defect, based on the $B_s+\{O_i\}_2$ model of Schmidt and Bothe,[27,29,34] has been recently described by Adey *et al.*[7] Upon exposure to band gap light, the $\{O_i\}_2$ dimers diffuses rapidly via the Bourgoin-Corbett mechanism with an activation energy calculated to be 0.3 eV, very close to the activation energy associated with the formation of the defect, 0.37 eV. The $\{O_i\}_2$ dimer traps at B_s and forms a $\{B_s,O_i,O_i\}$ complex, which has different configurations in the 0 and the +1 charge states. The metastable configuration in one charge state is the stable configuration in the other charge state, each by the same amount, 0.4 eV. The authors estimate the thermodynamic (0/+) level associated with this complex to be

in the range $E_c-0.5$ eV to $E_c-0.7$ eV, with their lower value close to the $E_c-0.41$ eV reported experimentally. The binding energy of this complex relative to B_s^- and $\{O_i\}_2^{++}$ located several sites apart in the same (144 host atoms) supercell was calculated to be 0.38 eV. This leads the authors to predict a dissociation energy of $0.38+0.86=1.24$ eV in the dark, where 0.86 eV is the calculated migration energy of $\{O_i\}_2^{++}$ in the absence of minority carriers. This dissociation energy is consistent with the value reported experimentally.[27,31]

III. METHODOLOGY

Our results are obtained from self-consistent, first-principles theory based on local density functional theory in 64 host atoms periodic supercells. The calculations are performed with the SIESTA code.[35,36] The exchange-correlation potential is that of Ceperley-Alder[37] as parametrized by Perdew and Zunger.[38] Norm-conserving pseudopotentials in the Kleinman-Bylander form[39] are used to remove the core regions from the calculations. The basis sets for the valence states are linear combinations of numerical atomic orbitals of the Sankey type,[40,41] generalized to be arbitrarily complete with the inclusion of multiple zeta orbitals and polarization states.[35] In the present calculations, double-zeta (two sets of s and p orbitals) for the B and O atoms and polarized double-zeta (add one set of d orbitals) for the Si atoms are used. The charge density is projected on a real space grid with an equivalent cutoff of 150 Ry to calculate the exchange-correlation and Hartree potentials. A $2\times2\times2$ Monkhorst-Pack k point sampling[42] is used to optimize the structures.

The geometries of all the plausible configurations involving B_s or B_i and O_i or $\{O_i\}_2$ are obtained with conjugate gradients. The binding energies at 0 K are calculated in the +1 charge state from the energies of the complexes and their dissociation products in separate cells. For $\{B_s,O_i,O_j\}$, $E_b(0\text{ K})=\{Si_{63},B_s,O_i,O_i\}^+ + \{Si_{64}\} - \{Si_{63},B_s^-\} - \{Si_{64},\{O_i\}_2^{++}\}$ is negative if energy is gained by forming the complex. In the case of interstitial boron, the dissociation products are O_i^0 and B_i^+. All these defects have spin 0. An estimate of the (thermodynamic) gap levels of the defects is obtained using interstitial carbon (C_i) as a marker, a method which predicts gap levels within 0.2 eV.[43]

The dynamical matrices are calculated at $k=0$ using linear response theory.[44,45] The quality of the matrices obtained in this manner is now well documented.[46–48] Our calculations ignore the long wavelength contribution to the dynamical matrix arising from the electric fields associated with charged defects.[49] These corrections to the phonon density of states would mostly cancel out when performing vibrational free energy differences. In addition to providing all the local and pseudolocal vibrational modes (LVMs and pLVMs, respectively), the knowledge of all the normal modes of the cell allows the construction of the phonon density of state $g(\omega)$ and therefore Helmholtz vibrational free energy F_{vib}.[13] This calculation is straightforward once $g(\omega)$ is known. This function is obtained by evaluating the dynamical matrix at 90 q points in the Brillouin zone of the supercell. Note that $F_{vib}(0\text{ K})$ is the total zero-point energy.

The difference in configurational entropy per complex[13] is $\Delta S_{config}=(k_B/[\{A,B\}])\ \ln(\Omega_{pair}/\Omega_{nopair})$, where $[\{A,B\}]$ is the number of complexes, and Ω_{pair} and Ω_{nopair} are the number of configurations with all possible complexes forming and with all complexes dissociated, respectively. We define $\{A,B\}$ to be "dissociated" when no B species is within a sphere of radius r_c of any A. The results are not very sensitive to the actual value of r_c which is only loosely related to a capture radius since it comes into the calculations only in the high temperature limit. The number of sites for A, B, and $\{A,B\}$ is known and the concentrations $[A]$ and $[B]$ are estimated from experiment. If $[A]$ is larger than $[B]$, the maximum number of complexes is $[\{A,B\}]=[B]$. Note that a real sample often has traps for the dissociation products A and/or B that are distinct from isolated A and/or B in a perfect crystal. Any such traps are ignored here.

IV. ACCEPTOR-OXYGEN COMPLEXES IN SI: THEORY

A. Results at $T=0$ K

We studied the symmetrically inequivalent configurations of B_s and $\{O_i\}_2$, or B_i and O_i or $\{O_i\}_2$ in the 0 and +1 charge states. As discussed in Refs. 7, 24, and 25 and summarized above, the relevant reactions are $B_s^-+\{O_i\}_2^{++}\rightarrow\{B_s,O_i,O_i\}^+$, $B_i^++O_i^0\rightarrow\{B_i,O_i\}^+$, and $B_i^++\{O_i\}_2^0\rightarrow\{B_s,O_i,O_i\}^+$. The interactions of B_s and O_i (which do not diffuse at the temperatures relevant here) lead to an unstable complex. Systematic conjugate gradient optimizations lead to four low-energy structures with comparable binding energies. In this section, the binding energies $E_b=\Delta U$ are potential energy differences and do not include zero-point energies. Mulliken population analyses show that all the structures described below involve threefold coordinated O atoms, with three nearly equal overlap populations of 0.3.

The reaction $B_s^-+\{O_i\}_2^{++}\rightarrow\{B_s,O_i,O_j\}^+$ leads to the formation of the structure shown in Fig. 2, with $E_b=0.54$ eV. The thermodynamic (0/+) level of this defect, calculated using C_i as a marker, is at $E_c-0.45$ eV. This value is very close to the experimental[30] value of $E_c-0.41$ eV. As pointed out earlier,[50] our configuration is different from the one of Adey *et al.*[7] who find O to be bound directly to B with $E_b=0.38$ eV and a (0/+) level in the range $E_c-0.5$ eV to $E_c-0.7$ eV. Our calculations predict that the Adey structure is barely stable. Recent calculations[51] confirm our result. Since the B_s-Si bond length is shorter than the Si-Si one, boron tends to pull its four nearest neighbors inward towards it. On the other hand, O_i resides at a puckered bond-centered sites and pushes its two Si neighbors away from it. Thus, with O_i bound to Si at a second nearest site to B, the two impurities help each other optimize their bond lengths and reduce the strain.

The reaction $B_i^++O_i^0\rightarrow\{B_i,O_i\}^+$ leads to he formation of the $\{B_i,O_i\}^+$ complex with C_{1h} symmetry and $E_b=0.47$ eV, shown in Fig. 3. Here again, O_i binds to Si rather than to B. The thermodynamic (0/+) level of this defect, calculated using C_i as a marker, is at $E_c-0.49$ eV. The experimental estimates for this level are in the range $E_c-0.23$ eV to $E_c-0.30$ eV, and our prediction is still within the 0.2 eV error

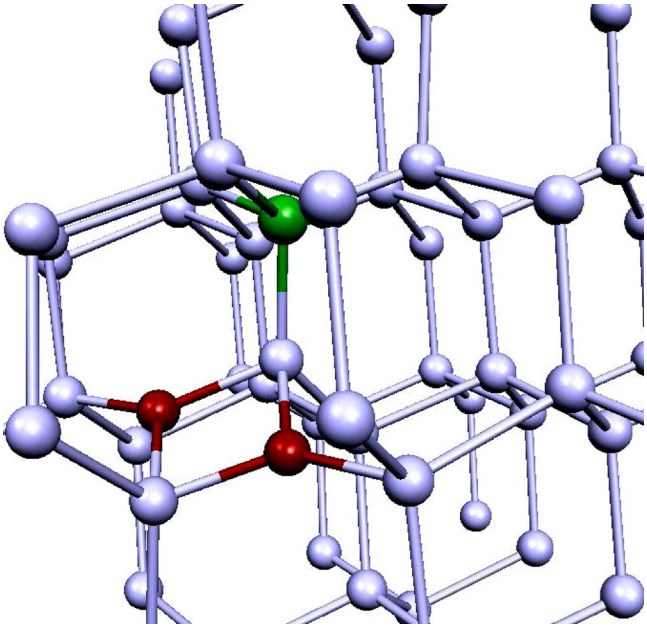

FIG. 2. (Color online) The lowest energy structure of the $\{B_s,O_i,O_i\}^+$ complex. The gray (green) ball is B, the two dark balls (red) are O, and the light gray (light blue) balls are the Si atoms.

bar associated[43] with the marker method for estimating thermodynamic gap levels. Note that "B_i" is a split-interstitial complex with B much closer to the substitutional site than Si. Adey *et al.*[24,25] predict a different configuration for this complex, with $E_b=0.6$ eV and gap level at $E_c-0.22$ eV. As mentioned above, we find their structure to be metastable, albeit very close in energy to ours. The existence of two configurations for the $\{B_i,O_i\}$ complex could explain why a rather wide range of gap levels ($E_c-0.23$ eV to $E_c-0.30$ eV) has been reported by various groups.

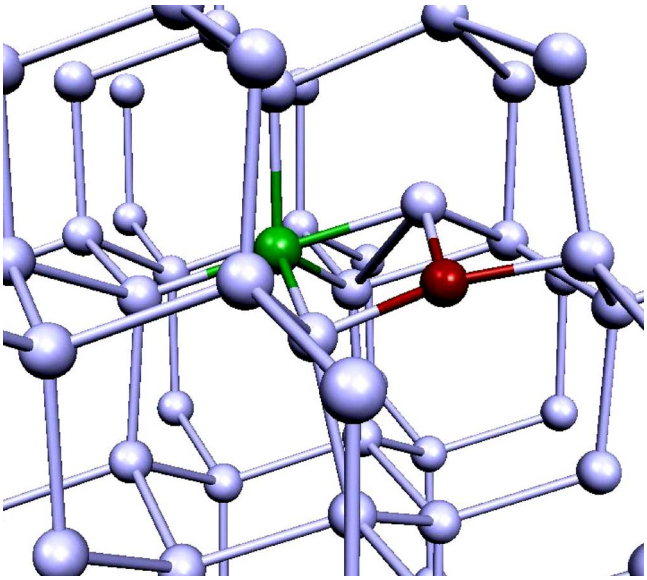

FIG. 3. (Color online) The lowest energy structure of the $\{B_i,O_i\}^+$ complex. The gray (green) ball is B, the dark ball (red) is O, and the light gray (light blue) balls are the Si atoms.

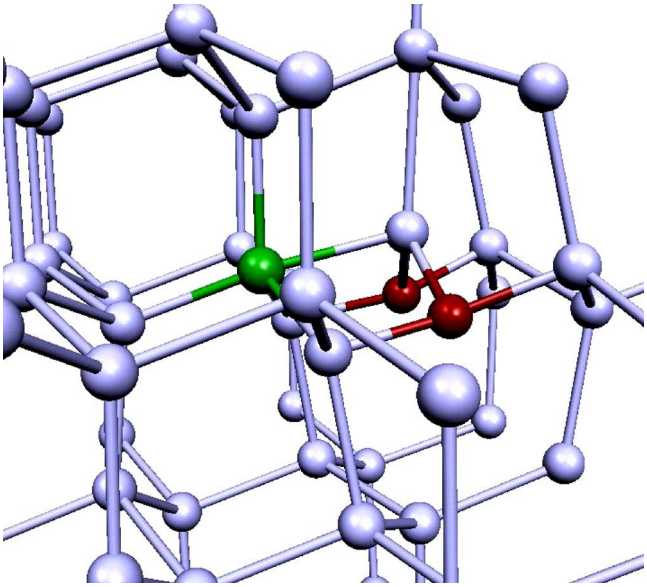

FIG. 4. (Color online) The $\{B_i,O_i,O_i\}_1^+$ complex. The gray (green) ball is B, the two dark balls (red) are O, and the light gray (light blue) balls are the Si atoms.

Finally, two nearly degenerate structures with $E_b=0.55$ eV and 0.61 eV, and $(0/+)$ levels at $E_c-0.54$ eV and $E_c-0.48$ eV, respectively, result from the reaction $B_i^+ + \{O_i\}_2^0 \rightarrow \{B_i,O_i,O_i\}^+$. These structures, labeled with the indices "1" and "2," respectively, are shown in Figs. 4 and 5. The latter has one O bound directly to B. Note that the low concentrations of both B_i and $\{O_i\}_2$ in the samples suggest that these two complexes have a low formation probability. Their binding energies and electrically active levels in the gap are com-

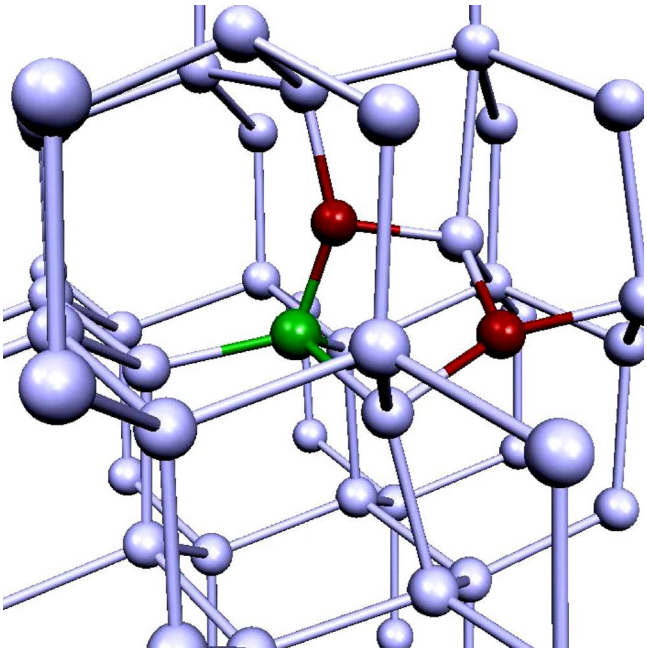

FIG. 5. (Color online) The $\{B_i,O_i,O_i\}_2^+$ complex. The gray (green) ball is B, the two dark balls (red) are O, and the light gray (light blue) balls are the Si atoms.

parable to those of the $\{B_s,O_i,O_i\}$ and $\{B_i,O_i\}$ defects. However, as will be shown in the next subsection, the thermal stability of both $\{B_i,O_i,O_i\}$ complexes is very low.

For completeness, we show in Fig. 6 the LVMs and pLVMs associated with the B and O atoms for the $\{B_s,O_i,O_i\}^+$ and $\{B_i,O_i\}^+$ complexes. Most of the modes involve the motion of several atoms and the following descriptions are approximate.

$\{B_s,O_i,O_i\}^+$: the 792 cm^{-1} mode has the two O atoms moving in opposite directions along the diagonal of the square; the 773 cm^{-1} mode is a Si-B stretch where Si is bound to both O atoms; the 686 cm^{-1} mode involves the motion of four atoms; the 669 and 625 cm^{-1} modes are B-Si stretch modes with symmetrically inequivalent host atoms; the 586 and 575 cm^{-1} modes are scissor modes involving both O atoms; the 271 cm^{-1} pLVM is a wag mode involving both O atoms.

$\{B_i,O_i\}^+$: the 833 cm^{-1} mode is the asymmetric stretch of O_i; the 688 cm^{-1} mode is a B-Si stretch; the 592 cm^{-1} mode involves substantial motion of O, B, and three Si atoms; the 575 cm^{-1} mode is also a B-Si stretch; the 550 cm^{-1} mode is a wag mode of B.

We calculated the same structures using Ga instead of B. The geometries are very similar but the binding energies much smaller: $E_b=0.12$ eV for $\{Ga_s,O_i,O_i\}^+$ and $E_b=0.09$ eV for $\{Ga_i,O_i\}^+$, respectively. As will be shown in the next section, these complexes are marginally stable at low temperatures while Ga and O repel each other above 200 K or so. This is consistent with the experimental observation that no O-related lifetime degradation occurs in Ga-doped solar cells.[23,33]

B. Finite temperature results

The only contributions to E_b relevant in the present case are the vibrational free energy and the configurational entropy. The (Helmholtz) vibrational free energy is calculated as described in Sec. III and Ref. 13. The configurational entropy includes the orientational degeneracies, but the largest contributions come from the concentrations of the various species involved. We discuss the reaction $\{B_i,O_i\}\rightarrow B_i+O_i$ in order to illustrate how we did the calculations.

We assume a sample with N substitutional sites, $[O_i]$ and $[B_i]$ interstitial oxygen and boron impurities, respectively. In a 1 cm^3 sample with $N=5\times10^{22}$ substitutional sites, the number of sites for B_s, split-interstitial sites for B_i and staggered or square configurations[7] for $\{O_i\}_2$ is 5×10^{22}, and the number of (puckered) bond-centered sites for O_i is 10^{23}. We chose $[B_s]$, $[O_i]$, $[\{O_i\}_2]$, and $[B_i]$ to be 10^{19}, 10^{18}, 10^{14}, and 10^{14}, respectively. The numbers depend on the sample, but these are realistic values which could correspond to an actual experimental situation. Note that some concentrations may change with temperature. For example, O_i becomes mobile around 450 °C leading to a decrease of $[O_i]$ and an increase of $[\{O_i\}_2]$. Such changes are ignored here.

At low temperatures, all the B_i's traps one O_i. Each B_i is a split-interstitial complex with B and Si sharing a substitutional site. Since the split-interstitial can be oriented along four equivalent directions, there are 4N possible configurations for B_i. Thus, the number of ways one can arrange $[B_i]$ interstitials around N sites is $(4N)!/[B_i]!(4N-[B_i])!$. There are 12 equivalent configurations for each $\{B_i,O_i\}$ complex, thus $12^{[B_i]}$ possibilities. The remaining $[O_i]-[B_i]$ interstitial oxygens are distributed among $2N-12[B_i]$ puckered bond-centered sites. This can be achieved in $(2N-12[B_i])!/([O_i]-[B_i])!(2N-[O_i]-11[B_i])!$ ways. Thus, the number of configurations for $\{B_i,O_i\}$ complexes is

$$\Omega_{pairs}=\frac{12^{[B_i]}(4N)!\,(2N-12[B_i])!}{[B_i]!\,(4N-[B_i])!\,([O_i]-[B_i])!\,(2N-[O_i]-11[B_i])!}.$$

At high temperatures, all the $\{B_i,O_i\}$ complexes are dissociated. We can arrange $[O_i]$ oxygens among 2N bond-centered sites in $(2N)!/[O_i]!(2N-[O_i])!$ ways. If $r_c=5$ Å, no boron is within a sphere of radius 5 Å of any oxygen, implying that 32 substitutional sites around each O_i are not allowed, and these correspond to 128 configurations for B_i. Thus, the B_i's are distributed among $4N-128[O_i]$ sites, which can be achieved in $(4N-128[O_i])!/[B_i]!(4N-128[O_i]-[B_i])!$ ways. Thus, the number of configurations at high temperatures is

$$\Omega_{nopairs}=\frac{(2N)!\,(4N-128[O_i])!}{[O_i]!\,(2N-[O_i])!\,[B_i]!\,(4N-128[O_i]-[B_i])!}.$$

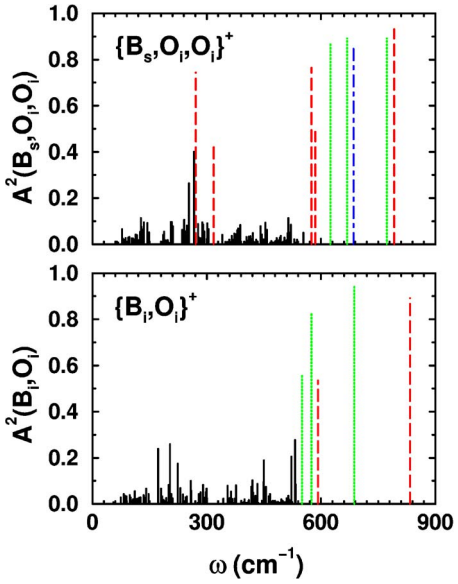

FIG. 6. (Color online) The square of the relative oscillation amplitude of the B and O atoms vs normal mode frequency for the $\{B_s,O_i,O_i\}^+$ (top) and $\{B_i,O_i\}^+$ (bottom) complexes. These amplitudes are obtained from the eigenvectors of the dynamical matrix. They do not include the dipole moment operator and are not IR intensities. The modes involving primarily B motion are the dotted (green) lines and the ones involving primarily O motion are the dashed (red) lines. The dashed-dotted (blue) line is a mode that has about equal oscillation amplitude of B and O. The modes are described in the text.

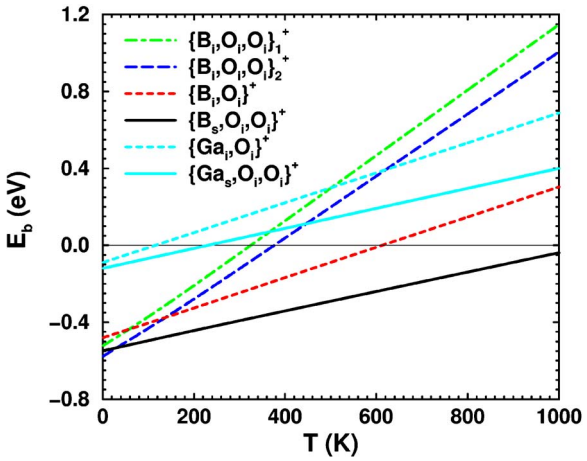

FIG. 7. (Color online) A binding free energies $\Delta E_b + \Delta F_{vib} - T\Delta S_{config}$ of the $\{B_s,O_i,O_i\}$, $\{B_i,O_i\}$, $\{B_i,O_i,O_i\}_1$, and $\{B_i,O_i,O_i\}_2$ complexes in Si. The free energies of the $\{Ga_s,O_i,O_i\}$ and $\{Ga_i,O_i\}$ complexes (light blue solid and dashed lines, respectively) start around -0.1 eV at $T=0$ K and are positive above 200 K.

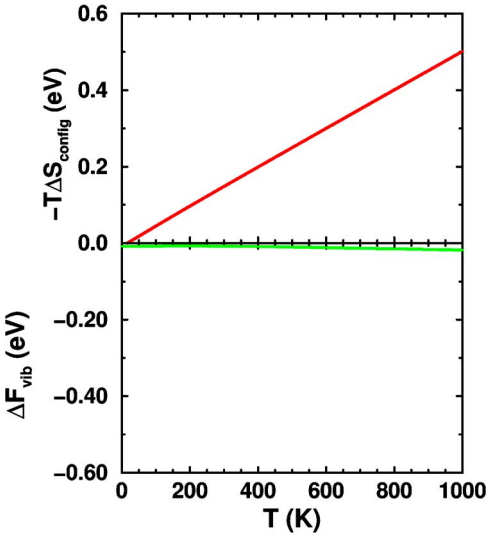

FIG. 8. (Color online) A comparison of ΔF_{vib} and $-T\Delta S_{config}$ terms in the binding free energy of the $\{B_s,O_i,O_i\}$ complex. Except near $T=0$ K where ΔF_{vib} has zero slope, both contributions are linear and the configurational entropy dominates.

Using Sterling's formula and an expansion for $\ln(1+\epsilon)$ with $\epsilon \ll 1$, we get

$$\Delta S_{config} = k_B\left(\ln\frac{6[O_i]}{N} - \frac{[B_i]}{[O_i]} - \frac{[B_i]}{4N}\right).$$

Similar calculations for $\{B_s,O_i,O_i\}$ (with a larger $r_c=10$ Å because of the Coulombic interaction) give

$$\Delta S_{config} = k_B\left(\ln\frac{12[B_s]}{N} + \frac{278[B_s]}{N} - \frac{[\{O_i\}_2]}{[B_s]}\right).$$

Finally, both configurations of $\{B_i,O_i,O_i\}$ have the same configurational entropy

$$\Delta S_{config} = k_B\left(\ln\frac{24[\{O_i\}_2]}{N} - \frac{[B_i]}{[\{O_i\}_2]}\right).$$

This gives $\Delta S_{config}=-0.515$, -0.778, and -1.538 meV/K for $\{B_s,O_i,O_i\}$, $\{B_i,O_i\}$, and $\{B_i,O_i,O_i\}$, respectively.

The difference between these situations is huge, and the reason for it is quite obvious. Consider an $\{A,B\}$ complex which dissociates into A and B. If A and/or B are abundant (as is the case for B_s and/or O_i), there are many configurations resulting in pairs and relatively few configurations with A away from B. On the other hand, when both A and B are scarce (as is the case for B_i and $\{O_i\}_2$), there are far fewer ways to make pairs and a great number of dissociated configurations. The binding free energies of the $\{B_s,O_i,O_i\}$, $\{B_i,O_i\}$, and $\{B_i,O_i,O_i\}_{1,2}$ complexes and their Ga analogues are plotted as a function of temperature in Fig. 7. None of the $\{Ga,O\}$ complexes are stable above ~200 K. Note that above some temperature T_0 where $E_b(T_0)=0$, the interactions become *repulsive*. For strongly bound complexes, this T_0 may well be above the melting point of the material, but in the present case, several of the complexes readily dissociate at moderate temperatures.

In all the binding free energies we have considered so far, the configurational entropy term dominates the temperature dependence at all but the lowest temperatures and the slope of $E_b(T)$ is very close to $|\Delta S_{config}|$. This is illustrated in Fig. 8 which compares ΔF_{vib} to $-T\Delta S_{config}$ for the $\{B_s,O_i,O_i\}$ complex. Note that in the harmonic approximation, ΔF_{vib} is a linear function of T, even though F_{vib} is not.

In good approximation, $E_b(T) \approx E_b(0) - T\Delta S_{config}$. If R is a dissociation rate, $R\exp\{-E_b/k_BT\} = R\exp\{\Delta S_{config}/k_B\}\exp\{-E_b(0)/k_BT\}$, and an Arrhenius plot yields a straight line with slope $-E_b(0)/k_B$ and intercept $(\ln R + \Delta S_{config}/k_B)$. Thus, Arrhenius plots of the dissociation of an $\{A,B\}$ complex in samples containing different concentrations of A and/or B produce parallel lines: the slopes are the same but the intercepts differ. This suggests a way to measure configurational entropies. If we take $R=10^{11}$ and $\Delta S_{config}=-0.5$ or -1.0 meV/K, the intercepts will be at $25.3-5.8=19.5$ or $25.3-11.6=13.7$, a measurable change.

C. Key results for acceptor-oxygen complexes

We have calculated from first principles the configurations, thermodynamic gap levels and binding energies of acceptor-oxygen complexes in Si. We find that the $\{B_i,O_i\}^+$ complex has two inequivalent configurations with similar binding energies. Our lowest-energy structure differs from that predicted earlier.[24,25] Our gap level is deeper than earlier predictions. Both configurations could be the defect(s) responsible for the lifetime degradation in irradiated (space based) solar cells. We agree with the key features of the $B_s^- + \{O_i\}_2^{++}$ interaction discussed in Ref. 7, but their structures (with O bound directly to B) are higher in energy than when O is at a second-nearest site to B_s (with O bound only to Si atoms). The key properties of the complex are very similar to the ones predicted earlier. We confirm that the $\{B_s,O_i,O_i\}$ complex is the defect responsible for the lifetime degradation in light-exposed (terrestrial) solar cells. We also find a metastable complex $\{B_i,O_i,O_i\}$ which has a larger

binding energy than the $\{B_i, O_i\}$ and $\{B_s, O_i, O_i\}$ complexes but is unstable above room temperature. Very similar structures are realized when Ga is substituted for B, but with smaller binding energies ($\sim$0.1 eV). These Ga-related complexes are unstable above 200 K or so.

V. DISCUSSION

We have calculated the binding free energies of four acceptor-oxygen complexes in Si, all of which have similar binding energies at $T=0$ K. The free energies were obtained from the (Helmholtz) vibrational free energies. The configurational entropies were calculated analytically with assumed impurity concentrations. The conclusions hold for any $\{A,B\}$ defect complex that dissociates into products A and B in any crystal. The key points are the following.

(1) The binding free energy of $\{A,B\}$ varies linearly with temperature with a slope largely dominated by the difference in configurational entropy between $\{A,B\}$ and A away from B.

(2) There is a temperature T_0 where $E_b(T_0)=0$. This temperature depends on the concentrations $[A]$ and $[B]$ and the binding energy at 0 K, $E_b(0)$. For $T>T_0$, the interaction between A and B becomes *repulsive*.

(3) The difference in configurational entropy depends on the concentrations $[A]$ and $[B]$ in the sample. Therefore, the binding free energy of a specific complex $\{A,B\}$ at a specific temperature will be different in samples containing different concentrations of A or B. In Arrhenius plots, this will appear to be a change in the dissociation rate but is really caused by a difference in ΔS_{config}.

(4) For a given $\{A,B\}$ complex, the smaller the concentration of A and B, the larger the configurational entropy associated with the dissociated species and the smaller the entropy associated with complex formation. Then, the slope of $E_b(T)$ is much steeper. The opposite holds if A and /or B exist in high concentrations. In the example discussed in this paper, changing one component of the complex from B_s to B_i changes the relevant concentration from 10^{19} to 10^{14}, which roughly triples ΔS_{config}.

(5) An Arrhenius plot of the dissociation reaction produces a straight line, the slope and intercept of which are very close to $-E_b(0)/k_B$ [not exactly because $E_b(T)$ is not linear at very low T] and $\ln R+\Delta S_{\text{config}}/k_B$ (not exactly because of a small contribution of ΔF_{vib}), respectively. Thus, a carefully controlled series of experiments could provide direct measurements of configurational entropy differences.

Finally, the role of the configurational entropy is critical when discussing dissociation-association reactions near the temperature T_0 where $E_b(T_0)=0$. This needs to be taken into account when discussing Ostwald or reverse Ostwald ripening processes, during which the concentration of isolated species and precipitates change substantially as a function of time. This affects the slope of $E_b(T)$ and therefore the value of T_0, which becomes time-dependent, and E_b can change sign. One would expect Ostwald ripening to occur for $T \ll T_0$ and more complicated dynamics for $T \sim T_0$.

ACKNOWLEDGMENTS

The authors are thankful to M. Stavola and A. A. Istratov for useful discussions. This work was supported in part by the National Renewable Energy Laboratory and the R. A. Welch Foundation.

*Electronic address: stefan.estreicher@ttu.edu

[1] A. M. Stoneham, *Theory of Defects in Solids* (Clarendon, Oxford, 1985).
[2] H. J. Queisser and E. E. Haller, Science **281**, 945 (1998).
[3] S. K. Estreicher, Mater. Today **6** (6), 26 (2003).
[4] *Oxygen in Silicon*, edited by F. Shimura, Semiconductors and Semimetals (1994), Vol. 42.
[5] J. Coutinho, R. Jones, P. R. Briddon, and S. Öberg, Phys. Rev. B **62**, 10824 (2000).
[6] Y. J. Lee, J. von Boehm, M. Pesola, and R. M. Nieminen, Phys. Rev. Lett. **86**, 3060 (2001).
[7] J. Adey, R. Jones, D. W. Palmer, P. R. Briddon, and S. Öberg, Phys. Rev. Lett. **93**, 055504 (2004).
[8] J. C. Bourgoin and J. W. Corbett, Phys. Lett. **38**, 135 (1972).
[9] M. von Smoluchowski, Z. Phys. Chem., Stoechiom. Verwandtschaftsl. **17**, 585 (1916).
[10] H. Reiss, C. S. Fuller, and F. J. Morin, Bell Syst. Tech. J. **35**, 535 (1956).
[11] J. I. Pankove and N. M. Johnson, in *Hydrogen in Semiconductors*, edited by J. I. Pankove and N. M. Johnson, Semicond. Semimetals **34**, 225 (1991).
[12] A. A. Istratov, H. Hieslmair, C. Flink, T. Heiser, and E. R. Weber, Appl. Phys. Lett. **71**, 2349 (1997).
[13] S. K. Estreicher, M. Sanati, D. West, and F. Ruymgaart, Phys. Rev. B **70**, 125209 (2004).
[14] I. Weinberg, S. Mehta, and C. K. Swartz, Appl. Phys. Lett. **44**, 1071 (1984).
[15] G. D. Watkins, Phys. Rev. B **12**, 5824 (1975).
[16] S. Zhao, A. M. Agarwal, J. L. Benton, G. H. Gilmer, and L. C. Kimerling, in *Defects in Electronic Materials II*, edited by J. Michel, T. Kennedy, K. Wada, and K. Thonke, Mater. Res. Soc. Symp. Proc. No. 442 (Materials Research Society, Pittsburgh, 1997), p. 231.
[17] R. D. Harris, J. L. Newton, and G. D. Watkins, Phys. Rev. B **36**, 1094 (1987).
[18] J. R. Troxell and G. D Watkins, Phys. Rev. B **22**, 921 (1980).
[19] P. M. Mooney, L. J. Cheng, M. Süli, J. D. Gerson, and J. W. Corbett, Phys. Rev. B **15**, 3836 (1977).
[20] P. J. Drevinsky *et al.*, in *Defects in Electronic Materials*, edited by M. Stavola, S. J. Pearton, and G. Davies, Mater Res. Soc. Symp. Proc. No. 104 (Materials Research Society, Pittsburgh, 1988), p. 167.
[21] H. Matsuura, Y. Uchida, N. Nagai, T. Hisamatsu, T. Aburaya, and S. Matsuda, Appl. Phys. Lett. **76**, 2092 (2000).
[22] M. Tajima *et al.*, IEEE Trans. Nucl. Sci. **48**, 2127 (2001).
[23] M. Tajima, M. Warashina, and T. Hisamatsu, *Proceedings of the 14th Workshop on Crystalline Silicon Solar Cells and Modules*, edited by B. L. Sopori (NREL, Golden, CO, 2004), NREL/BK-

520-36622, pp. 27–34.
[24] J. Adey, R. Jones, P. R. Briddon, and J. P. Goss, J. Phys.: Condens. Matter **15**, S2851 (2003).
[25] J. Adey, R. Jones, and P. R. Briddon, Appl. Phys. Lett. **83**, 665 (2003).
[26] J. Schmidt and A. Cuevas, J. Appl. Phys. **86**, 3175 (1999).
[27] J. Schmidt and K. Bothe, Phys. Rev. B **69**, 024107 (2004).
[28] S. W. Glunz, S. Rein, W. Warta, J. Knobloch, and W. Wettling, *Proceedings of the 2nd World Conference on Photovoltaic Energy Conversion* (European Commission, Ispra, Italy, 1998), p. 1343.
[29] J. Schmidt, K. Bothe, and R. Hezel, *Proceedings of the 29th IEEE Photovoltaic Specialists Conference* (IEEE, New York, 2002), p. 178.
[30] S. Rein and S. W. Glunz, Appl. Phys. Lett. **82**, 1054 (2003).
[31] S. Rein, T. Rehrl, W. Warta, S. W. Glunz, and G. Willeke, *Proceedings of the 17th European Photovoltaic Solar Energy Conference* (WIP-ETA, Munich, 2001), p. 1555.
[32] K. Bothe, R. Hezel, and J. Schmidt, Appl. Phys. Lett. **83**, 1125 (2003).
[33] S. W. Glunz, S. Rein, and J. Knobloch, *Proceedings of the 16th European Photovoltaic Solar Energy Conference* (WIP-ETA, Munich, 2000), p. 1.
[34] K. Bothe, R. Hezel, and J. Schmidt, Solid State Phenom. **95-96**, 223 (2004).
[35] D. Sánchez-Portal, P. Ordejón, E. Artacho, and J. M. Soler, Int. J. Quantum Chem. **65**, 453 (1997).
[36] E. Artacho, D. Sánchez-Portal, P. Ordejón, A. García, and J. M. Soler, Phys. Status Solidi B **215**, 809 (1999).
[37] D. M. Ceperley and B. J. Alder, Phys. Rev. Lett. **45**, 566 (1980).
[38] J. P. Perdew and A. Zunger, Phys. Rev. B **23**, 5048 (1981).
[39] L. Kleinman and D. M. Bylander, Phys. Rev. Lett. **48**, 1425 (1982).
[40] O. F. Sankey and D. J. Niklewski, Phys. Rev. B **40**, 3979 (1989); O. F. Sankey, D. J. Niklewski, D. A. Drabold, and J. D. Dow, Phys. Rev. B **41**, 12750 (1990).
[41] A. A. Demkov, J. Ortega, O. F. Sankey, and M. P. Grumbach, Phys. Rev. B **52**, 1618 (1995).
[42] H. J. Monkhorst and J. D. Pack, Phys. Rev. B **13**, 5188 (1976).
[43] J. Coutinho, V. J. B. Torres, R. Jones, and P. R. Briddon, Phys. Rev. B **67**, 035205 (2003).
[44] S. Baroni, P. Giannozzi, and A. Testa, Phys. Rev. Lett. **58**, 1861 (1987).
[45] X. Gonze and C. Lee, Phys. Rev. B **55**, 10355 (1997).
[46] J. M. Pruneda, S. K. Estreicher, J. Junquera, J. Ferrer, and P. Ordejón, Phys. Rev. B **65**, 075210 (2002).
[47] M. Sanati, S. K. Estreicher, and M. Cardona, Solid State Commun. **131**, 229 (2004); R. K. Kremer, M. Cardona, E. Schmitt, J. Blumm, S. K. Estreicher, M. Sanati, M. Bockowski, I. Grzegory, T. Suski, and A. Jezowski (unpublished).
[48] S. K. Estreicher, D. West, J. Goss, S. Knack, and J. Weber, Phys. Rev. Lett. **90**, 035504 (2003).
[49] S. Baroni, S. de Gironcoli, and A. Dal Corso, Rev. Mod. Phys. **73**, 515 (2001).
[50] M. Sanati and S. K. Estreicher, in *Proceeding of the 14th Workshop on Crystalline Silicon Solar Cell Materials and Processes*, edited by B. Sopori (NREL, Golden, CO 2004), NREL/BK 520-36622, p. 180.
[51] M.-H. Du, H. M. Branz, R. S. Crandall, and S. B. Zhang (private communication).